

# Warped Spectroscopy: Localization of Frozen Bulk Modes

---

Andrew R. Frey

California Institute of Technology  
Mail Stop 452-48  
Pasadena, CA 91125, USA  
frey@theory.caltech.edu

Anshuman Maharana

Department of Physics  
University of California, Santa Barbara  
Santa Barbara, CA 93106, USA  
anshuman@physics.ucsb.edu

**Abstract:** We study the 10D equation of motion of dilaton-axion fluctuations in type IIB string compactifications with three-form flux, taking warping into account. Using simplified models with physics comparable to actual compactifications, we argue that the lightest mode localizes in long warped throats and takes a mass of order the warped string scale. Also, Gukov-Vafa-Witten superpotential is valid for the lightest mass mode; however, the mass is similar to the Kaluza-Klein scale, so the dilaton-axion should be integrated out of the effective theory in this long throat regime (leaving a constant superpotential). On the other hand, there is a large hierarchy between flux-induced and KK mass scales for moderate or weak warping. This hierarchy agrees with arguments given for trivial warping. Along the way, we also estimate the effect of the other 10D supergravity equations of motion on the dilaton-axion fluctuation, since these equations act as constraints. We argue that they give negligible corrections to the simplest approximation.

**Keywords:** Flux Compactifications.

---

## Contents

1. Introduction	1
1.1 Toy Example	3
2. Geometry and Flux	8
3. Linearized Equations of Motion	11
3.1 Compensator Equations	11
3.2 Simplified Equation of Motion	14
3.3 Semiclassical Localization	17
3.4 More Detailed Models	18
4. Discussion	21
A. Estimate of Compensator Effects	24
B. Throat Plus Bulk Calculations	26

---

## 1. Introduction

A central theme in string phenomenology in recent years has been the study of compactifications in the presence of background fluxes. In these constructions, non-trivial quanta of form fields wrap cycles of the internal manifold, and "geometric flux" may introduce nontrivial bration structures. One of the attractive features of these constructions is that they help resolve the moduli problem in Calabi-Yau compactifications. With the introduction of flux, a large number of flat directions of the Calabi-Yau moduli space are lifted classically. As a result, the moduli acquire specific expectation values. With the loss of flat directions, the number of massless four dimensional scalars are reduced, helping make string compactifications more realistic.

In type IIB string theory, the work of Giddings, Kachru, and Polchinski [1] provides an algorithm to construct explicit solutions to equations of motion in the presence of fluxes. In these constructions, the geometry is a warped product with a conformal Calabi-Yau as the internal manifold. Imaginary-self-dual three-form flux threads the cycles of the Calabi-Yau, and these fluxes generically freeze the complex structure moduli of the Calabi-Yau as well as the dilaton-axion. Detailed studies of this phenomenon have been carried out in a large number of examples [2-7]. For reviews, see [8-10].

The four dimensional effective action governing the low energy dynamics of these compactifications is of much interest for a large number of phenomenological questions. However, at present we do not have a complete understanding of the dimensional reduction of these backgrounds; the warp factor gives rise to many complications [11-13]. Steps toward understanding the dimensional reduction were taken in [14], in which the equations describing linearized fluctuations were derived. A complete analysis was not possible because of two reasons. First, the equations are extremely complicated in the presence of regions of large warping. Second, the problem has the nature of an eigenvalue problem; that is, a solution involves finding both the mass and the wavefunction of the excitation.

Let us examine these issues in more detail. In the infinite volume limit, the warping is small in all regions of the spacetime and the linearized equations are easily analyzed. We find fluctuations of the complex structure moduli and dilaton-axion of mass suppressed by  $\ell^2/d^2$  compared to the Kaluza-Klein scale, where  $d$  is the linear scale of the compactification. The Kaluza-Klein wavefunctions of the metric perturbations are just the complex structure deformations of the Calabi-Yau, while the wavefunction of the dilaton-axion is a constant over the compactification.

However, at smaller volume, the compactification develops throats, regions of significant warping where the warp factor becomes nontrivial. Because the warp factor has nonvanishing derivatives along the compact directions, the linearized supergravity (SUGRA) equations of motion couple, so the fields in the four dimensional effective theory are actually mixtures of the SUGRA fluctuations. The extra SUGRA fields that are excited in a particular 4D modulus are called "compensators" [14], as they compensate for constraints imposed by the coupled equations. The warp factor also introduces position dependence to the fluctuation equations. Therefore, the true Kaluza-Klein modes (denoted "KK" modes) are actually mixtures of the naive Kaluza-Klein ("kk") modes of the unwrapped Calabi-Yau.

Given the interesting phenomenological applications of regions of large warping, it is important to understand Kaluza-Klein reduction in their presence. In this paper, we take some preliminary steps in this direction. Our focus is the dilaton-axion, which has the simplest equations of motion. To make the equations of motion tractable, we introduce some simplifications into the equations of motion and the geometry. While in agreement with our understanding of the infinite volume limit, our models suggest a qualitatively distinct behavior in the presence of deep throats. In particular, when the warped hierarchy between the top and bottom of the throat is large, the lowest mass mode of the dilaton has a mass given by the warped string scale, and its wavefunction is highly localized in the bottom of the throat. This mode is continuously connected to the lowest mode at infinite volume as the volume of the compactification is decreased, the wavefunction of the dilaton continuously varies from being uniformly spread over the internal manifold to a highly localized function. The fact that the lowest mode changes continuously as a function of the compactification volume modulus also implies that the Gukov-Vafa-Witten superpotential [15] applies to the lightest KK mode even when warping is important. We also find that the lightest mass is generically similar to the KK mass gap in the long throat regime, so the dilaton-axion should often be integrated out

of the effective theory, leaving a constant superpotential.

Our conclusions are similar to those of Goldberger and Wise [16], who discussed the dimensional reduction of a massive scalar in the Randall-Sundrum scenario [17]. In fact, our estimate of the mass in the long throat regime reproduces that of [16]. In the context of type IIB string compactifications, the Kaluza-Klein modes of the graviton exhibit a similar phenomenon [18–20], except that the lowest mode is massless and does not localize. Although we are unable to perform a systematic study, our analysis suggests that localization in long throats also occurs for the complex structure moduli of the underlying Calabi-Yau.

In outline, we next present a toy model which exhibits most of the key features of our analysis. Section 2 reviews some aspects of flux compactifications in type IIB string theory. The bulk of the paper is section 3, in which we first discuss the equations of motion for SUGRA fluctuations and argue that the compensators give negligible corrections to the mass. Then we introduce our simplified geometry in 3.2, reproducing the results of [16] and give a semiclassical analysis in 3.3. We then give results for compactification-like models in section 3.4. Finally, in section 4, we discuss various implications of our results and some future directions.

### 1.1 Toy Example

Consider the five dimensional spacetime

$$ds^2 = e^{2A(\varphi)} dx^\mu dx_\mu + d\varphi^2 \quad (1.1)$$

where the warping is a step function

$$\begin{aligned} A(\varphi) &= H; & 0 \leq \varphi \leq L & \quad (\text{region I}) \\ A(\varphi) &= 0; & L < \varphi \leq R & \quad (\text{region II}) : \end{aligned} \quad (1.2)$$

In this simplified model, region II is the analogue of the bulk in a string construction with fluxes, the part of the Calabi-Yau where the warping is insignificant. Region I represents a region of non-trivial warping; for  $H \gg 1$  and  $R \gg L$ , it can be thought of as a throat in the compactification.

We consider a scalar particle, of five-dimensional (5D) mass  $m_f$  (meaning “flux-induced mass,” as will be clear later), propagating in this spacetime with Neumann boundary conditions. We dimensionally reduce this scalar along the  $\varphi$  direction, particularly examining the wavefunction and masses of particle-like excitations in 4D as a function of  $H$  and  $m_f$ .

The equation of motion for the scalar is

$$\partial_\mu (e^{4A(\varphi)} \partial^\mu \phi) + e^{2A(\varphi)} \partial_\varphi^2 \phi(\varphi; \mathbf{x}) = e^{4A(\varphi)} m_f^2 \phi(\varphi; \mathbf{x}) : \quad (1.3)$$

For 4D particle excitations, the field decomposes as  $\phi(\varphi; \mathbf{x}) = \sum_n \phi_n(\varphi) u_n(\mathbf{x})$ , with  $\partial_\mu \phi = \sum_n \partial_\mu \phi_n(\varphi) u_n(\mathbf{x}) = m_n^2 \phi_n(\varphi) u_n(\mathbf{x})$ . Equation (1.3) then becomes

$$\frac{d}{d\varphi} (e^{4A(\varphi)} \frac{d\phi_n}{d\varphi}) + m_n^2 e^{2A(\varphi)} \phi_n = m_f^2 e^{4A(\varphi)} \phi_n : \quad (1.4)$$

In region I, this reads

$$\frac{d^2}{dx^2} \psi_n = (m_n^2 e^{2H} - m_f^2) \psi_n ; \quad (1.5)$$

and it becomes in region II

$$\frac{d^2}{dx^2} \psi_n = (m_n^2 - m_f^2) \psi_n : \quad (1.6)$$

This system is in many ways similar to the square well of one dimensional quantum mechanics. The solutions fall into two categories, solutions analogous of bound states with

$$m_n^2 e^{2H} - m_f^2 > 0 \text{ but } m_n^2 - m_f^2 < 0 \quad (1.7)$$

and the analogues of scattering states with

$$m_n^2 - m_f^2 > 0 : \quad (1.8)$$

Let us first examine the bound states. The equations of motion and the boundary conditions require  $\psi_n(x)$  to be of the form

$$\psi_n(x) = A \cos \sqrt{e^{2H} m_n^2 - m_f^2} x \quad (\text{region I}) \quad (1.9)$$

and

$$\psi_n(x) = B \cosh \sqrt{m_f^2 - m_n^2} (x - R) \quad (\text{region II}) : \quad (1.10)$$

Note that these modes have their wavefunction localized in region I and exponentially suppressed in the bulk. Therefore, we call these localized modes.

The masses  $m_n$  are obtained from the boundary conditions at the interface  $x = L$ . Continuity of the solution at the interface requires

$$\psi_n(L) = A \cos \sqrt{e^{2H} m_n^2 - m_f^2} L = B \cosh \sqrt{m_f^2 - m_n^2} (L - R) : \quad (1.11)$$

The matching condition for the derivative can be obtained by integrating (1.3) in a small neighborhood of the interface. We see that  $e^{4A(x)} \psi_n'(x)$  must be continuous; that is,

$$\frac{A e^{4H} \sqrt{e^{2H} m_n^2 - m_f^2} \sin \sqrt{e^{2H} m_n^2 - m_f^2} L}{B \sqrt{m_f^2 - m_n^2} \sinh \sqrt{m_f^2 - m_n^2} (R - L)} = \quad (1.12)$$

The ratio

$$\frac{e^{4H} \sqrt{e^{2H} m_n^2 - m_f^2} \tan \sqrt{e^{2H} m_n^2 - m_f^2} L}{\sqrt{m_f^2 - m_n^2} \tanh \sqrt{m_f^2 - m_n^2} (R - L)} = \quad (1.13)$$

of (1.12) and (1.11) then determines the masses. Although it is not possible to solve (1.13) analytically, we can develop a fairly good understanding of the spectrum by plotting the functions appearing on both sides of the equation. We begin by defining the variable

$$x = \sqrt{e^{2H} m_n^2 - m_f^2} L : \quad (1.14)$$

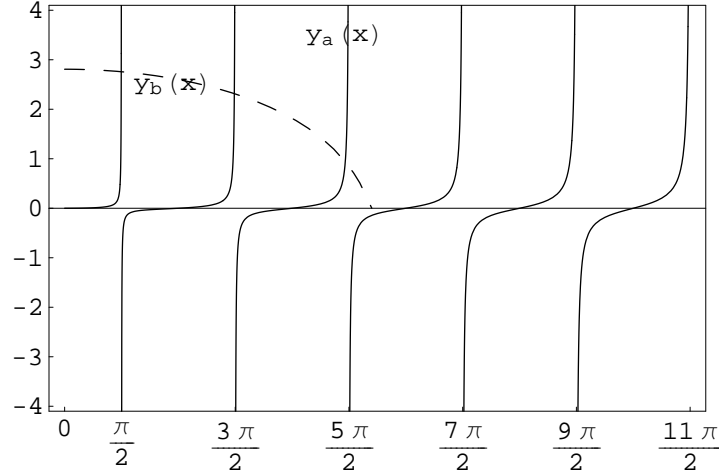


Figure 1: We can solve for the localized mode masses by finding intersections of the solid ( $y_a$ ) and dashed ( $y_b$ ) curves. The masses are given in terms of the intersection points  $x_n$  by equation (1.18). For illustrative purposes, we take  $m_f L = 3$ ,  $e^H = 3$ , and  $R=L = 2$ .

The left-hand side of (1.13) then represents the curve

$$y_a(x) = e^{4H} x \tan x ; \quad (1.15)$$

and the right-hand side is

$$y_b(x) = \frac{q}{m_f^2 L^2 (1 - e^{2H})} e^{2H} x^2 \tanh \frac{q}{m_f^2 L^2 (1 - e^{2H})} e^{2H} x^2 \frac{R}{L} - 1 : \quad (1.16)$$

The curve  $y_a(x)$  has a branch structure characteristic of  $\tan x$ , so  $y_a$  approaches infinity when  $x$  approaches odd multiples of  $\pi/2$ . On the other hand,  $y_b(x)$  is a squashed ellipse which intersects the  $x$ -axis at

$$x = L m_f \frac{\pi}{e^{2H}} : \quad (1.17)$$

Hence there is one intersection in each interval of  $\frac{\pi}{e^{2H}}$  on the  $x$ -axis for  $x < x_*$ , and we have  $\frac{e^H}{\pi} + 1$  localized modes.<sup>1</sup>

Now we can analyze the spectrum using (1.14), which can be written as

$$m_n^2 = e^{2H} m_f^2 \left( 1 + \frac{x_n^2}{m_f^2 L^2} \right) : \quad (1.18)$$

For a deep throat ( $e^H \gg 1$ ) with  $m_f^2 L^2 \gg 1$  (which is characteristic of throats in string compactifications), the lowest mode has mass

$$m_0 = m_f e^H : \quad (1.19)$$

<sup>1</sup>Note that, as in the square well problem in quantum mechanics, there is always at least one localized mode.

The highest mass for a localized mode is given by  $m_N = m_f$ , simply approximating  $x_N = \hat{x}$ . It is also important to consider the spacing of masses in order to determine whether there is a hierarchy between the KK mass scale and the flux-induced mass scale. For large masses  $m_n = m_f$ , we can show that

$$m_n = \frac{1}{L}; \quad (1.20)$$

which is the naive Kaluza-Klein scale of the throat. However, for light KK modes, near the lowest mass  $m_0 = e^H m_f$ , we find

$$m_n = \frac{e^H}{L}; \quad (1.21)$$

the warped Kaluza-Klein scale. In string compactifications, we will see that  $m_f$  and  $L$  are set by approximately the same quantum numbers and are larger than unity in string units, so  $m_n \propto m_f$  for small excitation number  $n$ . This is a crucial point for the validity of the flux superpotential in the 4D effective field theory. Also, we should note that the localized mode masses are practically independent of  $R$ , the volume of the bulk region, depending on it only weakly through  $x_n$ .

Next, we analyze the analogues of scattering states. For these, the Kaluza-Klein wavefunction takes the form

$$\psi_n(x) = A \cos \frac{q \sqrt{e^{2H} m_n^2 - m_f^2}}{e^{2H} m_n^2 - m_f^2} \quad (1.22)$$

in region I and

$$\psi_n(x) = D \cos \frac{q \sqrt{m_n^2 - m_f^2}}{m_n^2 - m_f^2} (R - x) \quad (1.23)$$

in region II. These solutions have an oscillatory profile in the bulk, so we call them bulk modes.

Again, the matching conditions at  $x = L$  determine the masses:

$$e^{4H} x \tan x = \frac{q \sqrt{e^{2H} x^2 - m_f^2 L^2 (1 - e^{2H})}}{e^{2H} x^2 - m_f^2 L^2 (1 - e^{2H})} \tan \frac{q \sqrt{e^{2H} x^2 - m_f^2 L^2 (1 - e^{2H})}}{e^{2H} x^2 - m_f^2 L^2 (1 - e^{2H})} - 1 = \frac{R}{L} \quad (1.24)$$

( $x$  is defined in terms of the mass as before). The left-hand-side of (1.24) is just the curve  $y_a(x)$  defined in (1.15). We add  $y_c(x)$ , a curve representing the right-hand-side of (1.24) to figure 1. Note that the condition  $m_n^2 > m_f^2$  requires us to consider only  $x > \hat{x}$ . See figure 2.

The spectrum of both localized and bulk modes can be inferred from figure 2. We would like to point out one important feature. Consider increasing the warped hierarchy  $H$  continuously, so the point  $\hat{x}$  toward the right along the  $x$ -axis. As a result, more and more bulk modes are smoothly converted to localized modes. The wavefunctions of the lower mass modes become highly localized in the region of significant warping. Also note that, for  $m_f = 0$ , there is a mode of zero mass and constant profile for all values of  $H$ . As  $m_f$  increases from zero, the wavefunction of this mode gradually localizes (for non-zero  $H$ ). The wavefunction of this lowest mass mode can always be written as a linear superposition of the eigenmodes at  $m_f = H = 0$  (since these form a complete set).<sup>2</sup> Since the lowest mode at

<sup>2</sup>These are just the naive KK modes and have the same wavefunctions for nonzero  $m_f$  and  $H = 0$ .

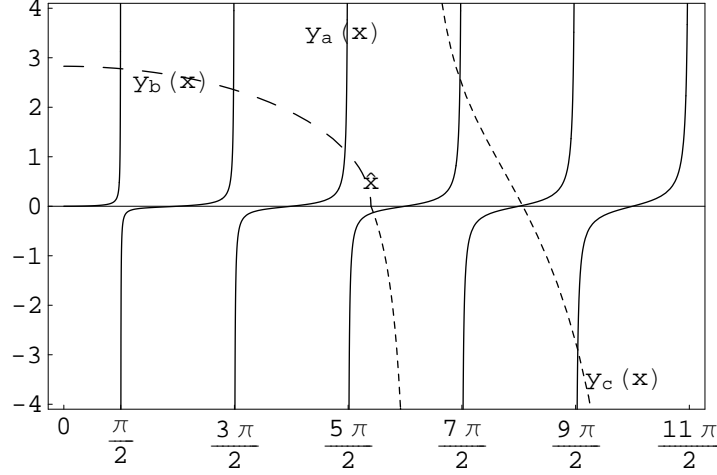


Figure 2: Plot showing all states in our example. The intersections of the dotted curve ( $y_c$ ) with the solid curve ( $y_a$ ) give the masses of the scattering modes.  $x$  indicates the cross-over between localized and bulk modes. The parameters of the model are as in figure 1.

$m_f; H = 0$  has a constant profile, any deviation of  $\phi_0(x)$  from a constant should be regarded as a mixing of the naive  $kk$  modes. Note that this mixing is energetically favorable, since it localizes the wavefunction in a region of large warping.

The idea of  $kk$  mode mixing suggests a treatment in perturbation theory. We can imagine two types of perturbation: perturbing around an unwarped background with finite  $m_f$  (that is,  $L e^H \neq 0$ ) or adding a perturbative mass  $m_f \neq 0$  to a warped background ( $L e^H$  finite). As it turns out, both of these perturbations are mathematically equivalent. For  $m_f^2 L^2 e^{2H} \ll 1$  (and  $R=L \ll 1$  for simplicity),

$$x_0^2 = m_f^2 L^2 e^{2H} \ll 1 \quad \frac{1}{2} e^{6H} m_f^2 L^2 e^{2H} \ll 1 \quad (1.25)$$

and

$$m_0 = m_f \ll \frac{1}{4} m_f^2 L^2 e^{8H} e^{2H} \ll 1^2 : \quad (1.26)$$

Even perturbatively, we see that the lightest mode becomes localized and has its mass reduced.

Finally, the astute reader may have noticed that we did not include the possibility of modes with  $m_n e^H < m_f$ . These would be supported by the matching conditions at  $x = L$  in much the same way that a delta-function potential can support a bound state and the same as the origin of the graviton zero mode in an RS compactification. However, the matching condition in that case would be

$$e^{4H} \left( \frac{q}{(1 - e^{2H}) m_f^2 + e^{2H}} \right) \tanh \left( \frac{q}{(1 - e^{2H}) m_f^2 + e^{2H}} \right) = \frac{q}{(1 - e^{2H}) m_f^2 + e^{2H}} \tanh \left( \frac{q}{(1 - e^{2H}) m_f^2 + e^{2H}} \right) \frac{R}{L} \ll 1 ; \quad (1.27)$$



where  $x$  as defined in (1.14) is now imaginary. Equation (1.27) has no solutions because the two sides have opposite sign, so there are no very light bound states. Note the contrast with the case of the graviton.

## 2. Geometry and Flux

In this section we review the compactifications of type IIB string theory constructed in [1]. Our treatment will be very brief, focusing on some specific features useful for our later discussion. For detailed and comprehensive reviews see [8{10].

In these constructions, the geometry<sup>3</sup> takes the form of a warped product

$$ds_{10}^2 = [e^{4A} + c]^{1=2} dx dx + [e^{4A} + c]^{1=2} g_{mn}(y) dy^m dy^n \quad (2.1)$$

where  $g_{mn}$  is the metric of a unit Calabi-Yau. The overall size of compactification is controlled by the parameter  $c$  (for details see [14]). For convenience, we will also denote  $e^{4\tilde{A}} = c + e^{4A}$  throughout this paper. In addition, there are nonzero components of  $R\text{-}R$  ( $F_3$ ) and  $NS\text{-}NS$  ( $H_3$ ) flux wrapping 3-cycles of the Calabi-Yau manifold. In the background compactification,  $G_3 = F_3 - H_3$  must be imaginary-self-dual on the Calabi-Yau, and this condition generically freezes the complex structure moduli as well as the dilaton-axion  $\tau = C + ie$ .

The warp factor  $e^{4A}$  satisfies a Poisson equation sourced by D 3-brane charge and 3-form flux

$$\tilde{\nabla}^2 e^{4A} = \frac{G_{mnp} G^{mnp}}{12 \text{Im}} + 2 \frac{1}{10} T_3 \tilde{\omega}_3^{\text{loc}}; \quad (2.2)$$

where the tilde indicates use of the underlying Calabi-Yau metric. In most parts of the manifold, the warp factor is approximately constant and the background resembles that of a standard Calabi-Yau compactification. This Calabi-Yau-like region is often referred to as the bulk. We have chosen conventions for the warp factor such that  $e^{4A} \rightarrow 0$  in the bulk; this convention is useful in that it makes clear the dependence of warping-induced hierarchies on the bulk volume modulus, of course the physically meaningful warp factor is given by  $\tilde{A}$ . We also note that (2.2) requires some source of negative D 3-brane charge, which can be provided by O 3-planes, O 7-planes, or F theory compactifications.

The reader should note that the metric (2.1) is not in a standard frame, since the external Minkowski metric is multiplied by a nontrivial constant in the bulk Calabi-Yau region. The massless graviton gives rise to a metric  $\hat{g}$  defined via

$$[1 + c^{-1} e^{4A}]^{1=2} \hat{g} = e^{2\tilde{A}} g \quad \hat{g} = c^{1=2} g; \quad (2.3)$$

We are used to dealing with the masses measured by  $\hat{g}$ , so the masses in this paper will be rescaled compared to our normal intuition by  $m = c^{1=4} \hat{m}$ . In other words, while the conventional mass of a Kaluza-Klein mode with trivial warping ( $e^{4A} = 0$ ) is  $\hat{m} = 1/c^{1=4} \hat{m}^0$ , we will have a Kaluza-Klein mass scale of  $m = 1/c \hat{m}^0$ . See also the discussion in [14].

---

<sup>3</sup>We shall use the 10D Einstein frame for our discussion and follow the conventions of [1].

In the bulk region, the flux is approximately constant at large volume. We define

$$\frac{1}{12} G_{mnp} G^{mnp} = \frac{1}{12} e^{6\tilde{A}} G_{mnp} G^{mnp} = \frac{n_f^2}{c^{3-0}} : \quad (2.4)$$

The explicit dependence on  $c$  arises due to the scaling of the metric with the overall volume. We have defined  $n_f^0$  as a sum over cycles of squares of flux quantum numbers,

$$n_f^0 = \sum_{RR} j_{RR}^2 + \sum_{NS} j_{NS}^2 : \quad (2.5)$$

In a general Calabi-Yau,  $j_{NS}^2$  will have some position dependence, but we expect the flux to be approximately constant except near shrinking 3-cycles. However, shrinking 3-cycles with wrapped flux will give rise to the throat regions described below, which we will describe separately from the bulk. The norm of the flux is important to us, as it induces a mass for the frozen moduli, including  $\tilde{c}$ .

In addition to the bulk of the Calabi-Yau, small regions of large ( $e^{4\tilde{A}} \sim c$ ) warping can arise from typical values of the flux quantum numbers, as shown in [1]. For instance, if  $M$  units of  $RR$  flux and  $K$  units of  $NS$ - $NS$  flux wrap the  $A$  and  $B$  cycles of a conifold locus respectively, the warp factor is exponential in the ratio of flux quanta:

$$e^{4\tilde{A}-0} = e^{g M/3K g_s} : \quad (2.6)$$

Such warped regions are called throats. The four dimensional energy of phenomenon localized in these regions is approximately redshifted by a factor of  $e^{\tilde{A}-0} c^{1=4}$  compared to modes in the bulk, making throats attractive for a whole host of phenomenological applications as indicated in [17,21]. This redshift factor is actually the ratio of  $e^{\tilde{A}}$  in the throat and the bulk; note that the redshift becomes of order one for  $c \sim e^{4\tilde{A}-0}$ . For larger  $c$ , the throat disappears entirely because  $e^{4\tilde{A}}$  contributes only a small perturbation around the value  $e^{4\tilde{A}-0} c$ . Therefore, we refer to the region  $c \sim e^{4\tilde{A}-0}$  as the infinite volume limit.

The local geometry in throats is of much interest to us. In these regions, the metric becomes independent of  $c$ , and the geometry is similar to that of the solution found in [22] (henceforth KS). The KS solution is a solution of the form (2.1) in which the Calabi-Yau  $\mathcal{M}_6$  in (2.1) is the non-compact deformed conifold. We note some features of this solution essential for our analysis and refer the reader to [22-25] for details. In this case, it is possible to solve for the warp factor explicitly. The warp factor  $e^{\tilde{A}}$  depends only on the radial direction of the conifold, and it attains its minimum value on the finite size  $S^3$  associated with the conifold deformation. The minimum value, which is that given in (2.6), is such that the proper size of the  $S^3$  in the warped metric is independent of the deformation parameter of the conifold. The radius of the  $S^3$  is approximately  $R_{S^3} = g_s^{1=4} M^{-1}$ .

In regions away from bottom of the throat, the geometry takes the form of a product  $AdS_5 \times T^{1,1}$  (up to logarithmic corrections in the warp factor), so

$$ds^2 = \frac{r^2}{R^2} dx dx + \frac{R^2}{r^2} dr^2 + R^2 ds_{T^{1,1}}^2 : \quad (2.7)$$

The AdS radius  $R$  (near which the throat connects to the bulk) is given by the effective three brane charge,  $R^4 = M K^{-2}$ . We model the KS throat by the metric (2.7) by restricting ourselves to  $r > r_0$  with

$$\frac{r_0}{R} = e^{A_0} \quad (2.8)$$

and choosing appropriate boundary conditions at  $r = r_0$  for fluctuating modes. This geometry with flux (and logarithmic corrections) was first discussed by Klebanov and Tseytlin [25] (henceforth KT). We will restrict our attention to this simplified KT model.

Let us now consider the flux in a KS throat. For a noncompact deformed conifold, the only flux components wrap the conifold A and B cycles. Just like in the bulk, the quantity  $G_{mnp}G^{mnp}$  is approximately constant in a KS throat (upto logarithmic corrections) for the A and B cycle fluxes, which follows directly from the solution for the flux in a KS background. This flux is also independent of the volume of the compactification due to the fact that geometry of the throat is practically independent of the bulk volume. However, with a compact Calabi-Yau attached to the KS throat, there are other possible flux components. These may have nonconstant  $\mathcal{F}_f$  in the throat, but we can assume that their norm is either constant or decreases in regions of small warp factor. Otherwise, they would alter the KS geometry significantly, possibly leading to a naked singularity. Therefore, as in the bulk case (2.4) above, we will define

$$\frac{1}{12}G_{mnp}G^{mnp} = \frac{1}{12}e^{6A}G_{mnp}G^{mnp} = \frac{n_f^2}{0}; \quad (2.9)$$

where  $n_f^2$  is a constant measuring the number of flux quanta (defined as in (2.5) above).

There are also other types of throats corresponding to flux wrapping cycles near other types of singularities, as described in [26]. In these throats, the metric takes the form (2.7) with  $T^{1,1}$  replaced by another Einstein-Sasaki manifold far from the bottom of the throat. The bottom of these throats (that is, the region with smallest warp factor) are expected to have a geometry similar to the bottom of the KS throat. Further, from studying the solutions in these throats, we see that we can write the flux norm as (2.9). Therefore, our results will apply to general throat regions in this class of compactification.

We close our review with a word on moduli stabilization. As we mentioned above, the requirement that  $G_3$  be imaginary-self-dual on the internal space generically implies that and the Calabi-Yau complex structure moduli must be fixed to specific values. Correspondingly, fluctuations around those vacuum expectation values are massive; in the 4D effective theory, it can be argued that those masses arise due to a superpotential

$$W = \int G_3 \wedge \hat{\cdot}; \quad (2.10)$$

where  $\hat{\cdot}$  is the holomorphic (3;0) form on the Calabi-Yau. From this superpotential, we see immediately that the frozen moduli must have masses  $\sim \mathcal{F}_f$ . In the following section, we will see from the linearized 10D equations of motion that a natural choice of mass scale is

what we will call the “flux-induced mass”

$$m_f^2(y) = \frac{g_s}{12} G_{mnp} G^{mnp}; \quad (2.11)$$

which generally will have some dependence on position in the compactification. In particular,  $m_f^2 \propto n_f^2$ , where  $n_f^2$  is the summed square of flux quantum numbers (as in (2.5)), which may differ in bulk and throat regions.<sup>4</sup> In a throat region, we have  $m_f \sim M_{\text{Pl}}^{\frac{1}{3}}$ , which is a bit bigger than unity in AdS units:  $m_f R \sim M_{\text{Pl}}^{\frac{1}{3}} M$ . Also, for typically Calabi-Yau manifolds,  $M$  cannot be too large due to a Gauss constraint on D3-brane charge. Finally, we note that [1] showed that the dilaton-axion and conifold deformation modulus cannot both be stabilized by the KS throat flux — additional components are necessary. In section 3.4, we will consider two different models for  $m_f(y)$  to take this fact into account.

### 3. Linearized Equations of Motion

In this section, we will first study the full linearized equations of motion for fluctuations of the dilaton-axion, arguing that they can be simplified to a lowest approximation. Then we give the simplified differential equation that we will take to govern the dilaton-axion’s Kaluza-Klein wavefunction.

#### 3.1 Compensator Equations

As was emphasized in [14] (and to a lesser extent in [3, 8]), the equations of motion of type IIB SUGRA mix the perturbative modes of many supergravity fields. Simply put, the field that corresponds to the dilaton-axion in the 4D EFT contains excitations of the 10D dilaton-axion along with many other SUGRA modes. The reason is that the dilaton-axion fluctuation appears as a source in the linearized equations of motion for the other SUGRA fields, which leads to constraint equations beyond the dynamical equation of motion. We are therefore forced to allow fluctuations of other SUGRA fields, which act as “compensators” for the dilaton-axion fluctuation. In this section, we will study the compensator equations for the dilaton-axion and argue that they give small corrections to the dilaton-axion dynamics.

The type IIB SUGRA equations of motion in 10D Einstein frame are

$$r^2 C = -2\partial_M \partial^M C - \frac{1}{6} e^2 F_{MNP} H^{MNP} \quad (3.1)$$

$$r^2 = e^2 \partial_M C \partial^M C + \frac{1}{12} e^2 F_{MNP} F^{MNP} - \frac{1}{12} e^2 H_{MNP} H^{MNP} \quad (3.2)$$

$$d\tilde{F}_5 = H_3 \wedge F_3 = H_3 \wedge \tilde{F}_3 \quad (3.3)$$

$$d(e \tilde{F}_3) = \tilde{F}_5 \wedge H_3 \quad (3.4)$$

$$d(e H_3 - e C \tilde{F}_3) = \tilde{F}_5 \wedge F_3 \quad (3.5)$$

---

<sup>4</sup>In our frame, the mass of a frozen modulus in the infinite volume limit is actually  $m_f = c^{1/4}$ ;  $m_f$  is instead the mass in the conventional frame.

along with the Einstein equations. We will proceed by linearizing these equations, starting with the dynamical equations (3.1,3.2) for the dilaton-axion. We will demonstrate that the 10D dilaton-axion cannot be the only fluctuations in a background with imaginary self-dual  $G_3 = F_3 - H_3$ . Let us consider an orientifold background for our flux compactification, in which the background dilaton-axion  $\tau = C + i\varphi_g$  is constant. With 03 and 07 orientifold planes, the dilaton-axion, metric, and 4-form potential fluctuations have even boundary conditions at the 0-planes, while both of the 2-form potentials have odd boundary conditions.

We define

$$\hat{F}_3 = F_3 - C H_3 ; \quad (3.6)$$

and we also note that

$$F_{mnp} H^{mnp} = 0 \text{ and } \frac{1}{2} G_{mnp} G^{mnp} = F_{mnp} F^{mnp} = \frac{1}{g_s^2} H_{mnp} H^{mnp} \quad (3.7)$$

due to the imaginary self-duality of the complex three form on internal space. In this type of background, the linearized equations of motion for the dilaton-axion are

$$\begin{aligned} \tilde{r}^2 - C &= \frac{g_s}{12} C G_{mnp} G^{mnp} - \frac{1}{6g_s} \hat{F}_{mnp} H^{mnp} + H_{mnp} F^{mnp} \\ &\quad - \frac{1}{2g_s} g_{mn} F^m{}_{pq} H^{npq} \\ \tilde{r}^2 &= \frac{g_s}{12} G_{mnp} G^{mnp} + \frac{g_s}{6} \hat{F}_{mnp} F^{mnp} + \frac{1}{g_s^2} H_{mnp} H^{mnp} \\ &\quad + \frac{g_s}{4} g_{mn} F^m{}_{pq} F^{npq} - \frac{1}{g_s^2} H^m{}_{pq} H^{npq} : \end{aligned} \quad (3.8)$$

Here  $g_{mn}$  is the complete change in the 6D metric, including any fluctuation in the warp factor, and the second line of each equation above indicates tree-level mixing between the dilaton-axion and internal metric fluctuations. This mixing appears in models with small numbers of flux components, for example [2,27]. From this point, we will neglect such mixing for simplicity.

Finally, splitting the Laplacian between internal and external dimensions and accounting for the warp factor,

$$\tilde{r}^2 + e^{4K} m^2 - \frac{g_s}{12} e^{4K} G_{mnp} G^{mnp} - C = e^{4K} \left( \frac{1}{6g_s} \hat{F}_{mnp} H^{mnp} + H_{mnp} F^{mnp} - \frac{g_s}{6} \hat{F}_{mnp} F^{mnp} - \frac{1}{6g_s} H_{mnp} H^{mnp} \right) ; \quad (3.9)$$

where  $m$  is the mass in the 4D EFT. Tildes indicate use of the underlying Calabi-Yau metric  $g_{mn}$ . The left-hand side of this equation (when set to zero) is the naive equation of motion for the dilaton-axion zero-mode in 3-form flux. The right-hand side indicates mixing with fluctuations of the 3-form flux, even though those fluxes are not naive KK zero-modes due to the orientifold projection.

With a trivial warp factor, the dilaton-axion zero-mode is the naive KK zero mode (that is, constant), and it does not mix with the 3-form fluctuations.<sup>5</sup> However, with nontrivial warping, the flux term on the left-hand side is position dependent, even on a torus with constant flux.<sup>6</sup> Therefore, the naive KK modes of the dilaton-axion must mix with each other, and the dilaton-axion further mixes with naive KK excitations of the 3-form flux. In that light, we should examine the other equations of motion. The 5-form equation linearizes to

$$d\tilde{F}_5 = H_3 \wedge \tilde{F}_3 + H_3 \wedge \tilde{F}_3 ; \quad (3.10)$$

so the 5-form perturbations are sourced if the 3-form perturbations are. Without writing out the full Einstein equations, we can also say that the warp factor must also be modified at the linear level in order for dilaton-axion perturbations to solve the equations of motion.

We will look at the 3-form equations in a little more detail. Using the fact that the background flux is constant, we can simplify the linearized equations to

$$\begin{aligned} d\tilde{F}_5 - g_s^{-1} H_3 + g_s^{-1} H_3 - g_s C \tilde{F}_3 + g_s^{-1} d(\tilde{F}_3) H_3 &= \tilde{F}_5 \wedge \tilde{F}_3 - \tilde{F}_5 \wedge \tilde{F}_3 \\ g_s d\tilde{F}_3 - C H_3 - C H_3 + g_s d(\tilde{F}_3) &= \tilde{F}_5 \wedge H_3 + \tilde{F}_5 \wedge H_3 : \end{aligned} \quad (3.11)$$

The change in the Hodge duality rule  $(\tilde{F}_3)$  embodies both fluctuations in the unwarped metric and the warp factor. Every possible fluctuation is involved in these equations, and there is not a simple solution, just as has been seen in other cases [3, 8, 14].

In order to estimate the effect of the compensators on the dilaton-axion zero-mode, we consider a simplified system. We stress that we are not attempting to solve the compensator equations but rather are studying a truncation of them as a rough guide to their effects. First, we take all fluctuations to vanish except for  $\tilde{F}_3$ ,  $\tilde{F}_3$ , and  $H_3$ . This choice is appropriate because the 3-form fluctuations appear directly in the dilaton-axion equations (3.9). With some massaging, we can then write (3.11) as

$$\begin{aligned} d\tilde{F}_3 - (dC) \tilde{F}_3 &= \frac{1}{g_s} H_3 \tilde{F}_5 \\ d\tilde{F}_3 - 2(dC) \tilde{F}_3 - g_s^2 (dC) \tilde{F}_3 &= g_s \tilde{F}_3 \tilde{F}_5 ; \end{aligned} \quad (3.12)$$

where

$$(pY^q)_{N_1 \dots N_{q-p}} = \frac{1}{p!} M_1 \dots M_p M_1 \dots M_p N_1 \dots N_{q-p} : \quad (3.13)$$

The next simplification we consider is to specify the geometry we consider; we will take a KS throat approximated by the KT metric (2.7) of  $AdS_5 \times T^{1,1}$  and further approximate  $T^{1,1}$  as  $S^3 \times S^2$ . We can reduce the dilaton-axion equation (3.9) to a 5D by taking the dilaton-axion to depend only on the external directions and the radial dimension  $r$ . Since we want

<sup>5</sup>We are approximating the norm of the flux  $G_{mnp} G^{mnp}$  to be constant on a large volume Calabi-Yau.

<sup>6</sup>However, it is possible to use the supersymmetry variations to argue that the dilaton-axion zero mode is constant for any warp factor in the absence of flux.

to keep the system of equations 5D, we should also take the 3-form fluctuations constant on the spheres. Then spherical symmetry suggests that we take

$$B = (x; r); \quad C = (x; r) \quad (3.14)$$

as the only nontrivial components of the NS-NS and R-R 2-form potentials. Here  $x$ ;  $r$  are the coordinates of the  $S^2$ . Finally, we truncate the equations of motion to (3.9) and the  $\hat{B}$  component of (3.12). In this simplified background, there are a number of cancellations, and the equations of motion become (in the NS-NS sector)

$$\begin{aligned} \partial_r^2 + \frac{5}{r} \partial_r - m_f^2 \frac{R^2}{r^2} + m_B^2 \frac{R^4}{r^4} \hat{B} &= \frac{1}{6g_s} \frac{n_h}{r} \partial_r \hat{B} \\ \partial_r^2 + \frac{5}{r} \partial_r + m_B^2 \frac{R^4}{r^4} \hat{B} &= \frac{n_h}{R} \frac{r}{R} \partial_r \hat{B}; \end{aligned} \quad (3.15)$$

and the R-R fields satisfy the similar equations

$$\begin{aligned} \partial_r^2 + \frac{5}{r} \partial_r - m_f^2 \frac{R^2}{r^2} + m_B^2 \frac{R^4}{r^4} \hat{C} &= \frac{1}{6g_s} \frac{n_h}{r} \partial_r \hat{C} \\ \partial_r^2 + \frac{5}{r} \partial_r + m_B^2 \frac{R^4}{r^4} \hat{C} &= \frac{n_h}{R} \frac{r}{R} \partial_r \hat{C}; \end{aligned} \quad (3.16)$$

Here, the number  $n_h$  is defined by  $H_r = n_h R^2 = r$ , which is the appropriate behavior for the NS-NS flux in a KS throat, and we have written the shorthand  $m_f^2$  as in (2.11). We have also defined  $\hat{B} = B = R^2$  and  $\hat{C} = C = R^2$  to make all our fields dimensionless.

We have solved the equations (3.15), treating the right-hand-sides as perturbations. Our results show that this approach is self-consistent; for example, when the full hierarchy of the KS throat is  $10^3$  and reasonable values are taken for compactification parameters, the change in mass-squared of the dilaton is about 1 part in  $10^4$ . Furthermore, from our numerical estimates, it appears that  $j(m^2)j \sim e^{A_0} m^2$ , where  $e^{A_0}$  is the minimum warp factor of the throat. Note that we have assumed that  $c = 0$  in modeling the throat as  $AdS_5 \times T^{1,1}$ ; in a more realistic compactification, we expect the compensators to give a negligible contribution in the bulk region. See the discussion above equation (3.10). See appendix A for more details of our estimate.

### 3.2 Simplified Equation of Motion

For simplicity, we approximate that the internal metric factorizes into a radial direction and 5D part, much as in the  $AdS_5 \times T^{1,1}$  KT geometry, and we take

$$ds^2 = dr^2 + L^2 [e^{4A} + c]^{1/2} ds_5^2 = dr^2 + L^2 e^{2\tilde{A}} ds_5^2; \quad (3.17)$$

where  $ds_5^2$  may be defined piecewise along the  $r$  direction. Here,  $L$  is the linear scale of the 5 "angular" dimensions; in the  $AdS_5 \times T^{1,1}$  background,  $L = R$ , the AdS radius.

The dilaton-axion equation of motion involves the scalar Laplacian of  $g_{mn}$ , which is

$$\tilde{r}^2 = \partial_r^2 + 5\partial_r A \partial_r + \frac{1}{L^2} e^{2A} r^2 \quad (3.18)$$

on any scalar  $\phi$ . We can find this relation simply using formulae for conformal scaling of the metric. Therefore, ignoring compensators, which give only a small correction, the dilaton-axion equation of motion becomes<sup>7</sup>

$$\partial_r^2 + 5\partial_r A \partial_r - e^{2A} \frac{Q^2}{L^2} - e^{2A} m_f^2 + e^{4A} m^2 = 0 : \quad (3.19)$$

Here,  $Q^2$  is defined as eigenvalue of the fluctuation with respect to the 5D Laplacian. Since we have oversimplified the full compactification geometry, it may be necessary to define  $A$  and  $Q$  in a piecewise manner over the range of  $r$ . Also,  $m_f$  is a function of  $r$  in the most general situation. However, if the warping is just a Randall-Sundrum (AdS<sub>5</sub>) throat, the differential equation reduces to the left-hand-side of (3.15) above, with the addition of angular momentum :

$$\partial_r^2 + \frac{5}{r} \partial_r - m_f^2 + \frac{Q^2}{L^2} - \frac{R^2}{r^2} + m^2 \frac{R^4}{r^4} = 0 : \quad (3.20)$$

At points where the definition of the warp factor or angular momentum are discontinuous, (3.19) yields the boundary conditions

$$; e^{5A} \partial_r \phi \text{ continuous} : \quad (3.21)$$

It is useful to recast the equation of motion (3.19) into a Schrodinger-like form, as has been done in the Randall-Sundrum case for graviton KK modes [17,28,29]. It is a simple matter to write

$$(\partial_x^2 + V(x)) \psi(x) = m^2 \psi(x) \quad (3.22)$$

for

$$dx = e^{2A} dr ; \quad \psi = e^{3A/2} \phi ; \quad (3.23)$$

and potential

$$V(x) = e^{3A/2} \partial_x^2 e^{3A/2} + e^{2A} m_f^2 + \frac{Q^2}{L^2} : \quad (3.24)$$

Note that the sign and integration constant in the definition of  $x$  (3.23) may be chosen for convenience (and to make  $x$  continuous if the warp factor is defined only piecewise continuously).

To build some intuition, we begin by considering a simplified KT model for the fluctuations of the dilaton. We consider its propagation in a finite domain  $r_0 < r < r_c$  of AdS<sub>5</sub>  $T^{1,1}$ , with  $r_0 = R = e^{A_0}$  and  $r_c^2 = R^2 = 1 = \frac{p}{c} \bar{c}$ . Then we have  $x = R^2 = r$  and a hierarchy in the throat of  $e^H$   $x_0 = x_c = e^{A_0} = c^{1/4}$ . We incorporate the effects of the infrared throat region and the

---

<sup>7</sup>This decomposition goes into the calculation of (3.15,3.16) as well.



bulk by imposing Neumann boundary conditions on  $\phi$  at both ends  $\pm r_c$ . In this approximation, we effectively have a RS model with five additional dimensions. For simplicity, we take  $m_f$  to be a constant. Our treatment, therefore, just becomes mathematically equivalent to that of Goldberger and Wise [16]. (We shall address the issue of varying  $\phi$  in sections 3.3 and 3.4.) The potential is

$$V(x) = \frac{1}{x^2} - \frac{15}{4} + m_f^2 R^2 + Q^2 \quad ; \quad (3.25)$$

With this potential, the Schrodinger equation (3.22) is a well-known form of the Bessel equation, with (unnormalized) solution

$$\psi(x) = \frac{r}{R} J\left(\frac{x}{R}\right) + b \frac{r}{R} Y\left(\frac{x}{R}\right) ; \quad Q = \frac{q}{4 + Q^2 + m_f^2 R^2} \quad ; \quad (3.26)$$

(Note that this solution is only valid for a nonzero mass,  $m_f \neq 0$ .) The boundary conditions can then be used to obtain an equation for the masses,

$$\begin{aligned} 2J(z_n) + z_n J^0(z_n) - 2Y(z_n)e^H + z_n e^H Y^0(z_n) \\ 2Y(z_n) + z_n Y^0(z_n) - 2J(z_n)e^H + z_n e^H J^0(z_n) = 0 ; \end{aligned} \quad (3.27)$$

where  $z_n = x_0 m_n$ . For large hierarchy ( $H \gg 1$ ), the condition (3.27) simplifies to

$$z_n - 2J(z_n) + z_n J^0(z_n) = 0 \quad (3.28)$$

for the lowest mass modes. Note that the prefactor, which arises from the Bessel Y functions, prevents  $z = 0$  from being a root, which is consistent because the Bessel function solution is not valid for a massless mode. (When  $Q = 0$  and  $m_f = 0$ , we know there should be a massless mode; this mode arises from the solution  $\phi \propto x^{3/2}$  | constant | for the potential (3.25). As shown in [16], this lowest mode gains a mass in perturbation theory as  $m_f$  increases from zero.)

The lowest mass mode has  $Q = 0$ . As it turns out, the lowest root of (3.28) is of the order of  $\pi$ , so

$$m_0 \approx \pi m_f = \frac{r_0}{R} m_f \quad ; \quad (3.29)$$

The reader may question how we know that the mass of this lowest mode is proportional to  $m_f$ . Actually, this is straightforward to check numerically for moderate values of the flux and large hierarchy (for example, we can calculate the derivative of the mass with respect to  $\phi$ ). Also, the profile of the lowest-mass mode is highly localized in the region close to  $r_0$ .

The separation of the roots of (3.28) is also of the order of unity; hence, the mass scale of the Kaluza-Klein tower is

$$m_{KK} \approx \frac{r_0}{R^2} \quad ; \quad (3.30)$$

Modes with angular momentum on the  $T^{1,1}$  directions also have energy given by the same scale. From our discussion in section 2, we note that  $R m_f \ll 1$ , so the lowest mass is about as large as the KK mass gap. Thus, the lowest mass mode of a massive bulk scalar (such as the dilaton-axion) must be integrated out along with the higher KK modes for a large class of applications.

### 3.3 Sem iclassical Localization

Next, we would like to discuss the localization of modes in more general settings. We can see when localization occurs in a rough semiclassical approximation using the Schrodinger-like equation (3.22). Using the effective potential, we can also discuss the effects of the variation of the flux induced mass term in the equation of motion of the dilaton. Recall that the potential is given by (3.24) as

$$V(x) = e^{3A-2} g_x^2 e^{3A-2} + e^{2A} m_f^2(x) + \frac{Q^2}{L^2} ; \quad (3.31)$$

where  $m_f(x)$  measures the magnitude of the flux in the warped geometry and  $Q$  measures the angular momentum of the KK mode in the other 5 dimensions of the compact manifold. Most qualitative features of the spectrum can be inferred from the structure of  $V(x)$ .

As an illustration, consider a pure  $AdS_5$  throat, as in the KT geometry. The potential (3.25) is inverse square and has a global minimum at  $x_0 = R^2 = r_0$ , the infrared end of the warped extra dimension. We would then expect the low lying modes to have masses at the scale set by the value of the potential at this minimum. This indeed is the case as can be seen from the results of our explicit computation, equations (3.29) and (3.30). That is, the dilaton zero-mode has a mass scale  $m_{A^0} = m_f R = x_0$ .

We are now ready to incorporate the effects of the variation of the flux term. For the lowest mode the relevant terms in the potential are the terms involving the warp factor and the flux induced mass term. Note that the potential  $V(x)$  is a local function of the warp factor and the fluxes. The parameters of our  $AdS_{T^{1,1}}$  model describe the throat region accurately; thus, even in the case of a realistic warp factor and flux-induced mass terms, the potential in the throat region is given by

$$V_{\text{throat}}(x) = \frac{1}{x^2} - \frac{15}{4} + m_f^2 R^2 : \quad (3.32)$$

In the bulk region, the derivatives of the warp factor are small, and the dominant contributions arises from the second term in (3.24). From our discussion of the bulk geometry and fluxes in section 2 it is easy to see that

$$V_{\text{bulk}}(x) = \frac{m_f^2}{c^{1/2}} = \frac{n_f^2}{0c^2} : \quad (3.33)$$

Comparing this with the value of (3.32) at its minimum, we conclude that the global minimum of the potential is in the infrared end of the throat if  $e^{A^0} = 1 = c$ . On the other hand, if  $e^{A^0} = 1 = c$ , then the minimum of the potential is in the bulk.

To summarize, our models suggest that the flux induced mass for the dilaton is determined by an interplay between the parameter  $c$  (which controls the overall volume) and  $e^{A^0}$  (the minimum value of the warp factor). In order to understand this competition, it is useful to start in the infinite volume limit ( $c = e^{4A^0}$ ) and decrease  $c$  adiabatically. In the infinite volume

lim it, the dilaton acquires a mass

$$m_{\frac{m_f^0}{c}} = p \frac{n_f^0}{g_s p_{=0_c}} ; \quad (3.34)$$

and its wavefunction in the internal directions is approximately constant. This is a roughly string scale mass (since  $n_f^0$  is not very large), suppressed by a volume factor.

Now consider decreasing the parameter  $c$ . For  $c \rightarrow e^{4A_0}$ , the geometry begins to develop a throat region. As  $c$  decreases further, the throat becomes more and more distinct. In this process, the wavefunction and mass of the dilaton also vary continuously. For  $c \rightarrow e^{A_0}$ , a qualitatively distinct behavior sets in. The dilaton-axion wavefunction becomes highly localized, and the mass is

$$m_{m_f e^{A_0}} = p \frac{n_f}{g_s p_{=0}} e^{A_0} : \quad (3.35)$$

This mass is approximately the warped string scale. The mass formulae (3.34) and (3.35) agree for  $c \rightarrow e^{A_0}$ , suggesting a smooth interpolation between the two regimes. In fact, as we will see in section 3.4 below, this semiclassical reasoning can fail in the regime

$$e^{A_0} \ll c \ll e^{4A_0} : \quad (3.36)$$

Finally, we would like to make some comments on mixing between zero-modes and naive  $kk$  modes encountered in the linearized analysis of [14]. At large volume, the lowest mass wavefunctions are given by the zero-modes of the Calabi-Yau. On the other hand, in the deep throat regime, the wavefunctions are localized. A Fourier decomposition of such a function in terms of the eigenmodes of the underlying Calabi-Yau ( $\mathfrak{g}_{mn}$ ) will involve non-trivial contributions from  $kk$  modes. This picture seems consistent with the strong mixing between zero-modes and  $kk$  modes found in [14] while examining massive fluctuations in the presence of deep throats. The effect of these  $kk$  modes is to localize the wavefunctions in the region of large warping, an energetically favorable process.

### 3.4 More Detailed Models

In the discussion of section 3.2, we modeled the bulk by imposing boundary conditions at  $r = r_c$ . However, we would be remiss if we did not explicitly add a region of constant warp factor representing the bulk. The model then becomes similar to the toy example discussed in the introduction.

The metric is of the general form (2.1) with the simplification (3.17), as before, with an  $AdS_5$  warp factor  $e^A = r=R$  dominating in a throat region and a constant warp factor in the bulk region. In summary,

$$e^{A^c} = c + e^{4A} \quad \text{for } r < r_c \quad \text{and} \quad e^A = r=R \quad \text{for } r_c < r < r_c + p_{=0} : \quad (3.37)$$

For continuity of the warp factor, we demand  $r_c=R = c^{1/4}$ , as in section 3.2. Also as before,  $e^{A_0} = r_0=R$  and  $e^H = e^{A_0} = c^{1/4}$ . The proper length of the bulk region is  $c^{1/4} p_{=0}$ , consistent

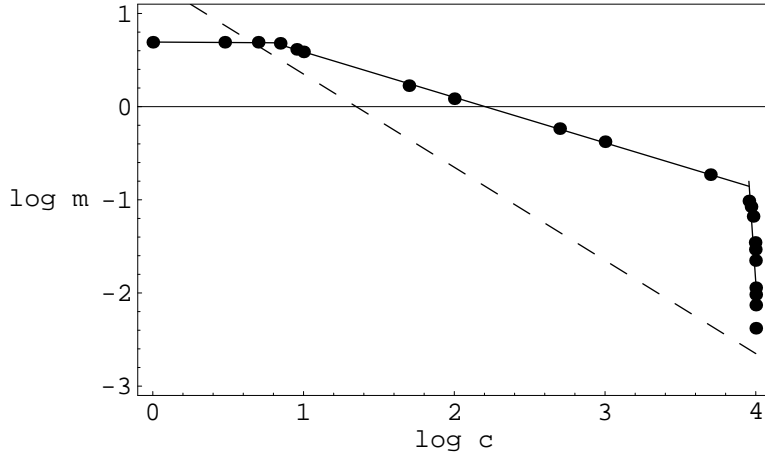


Figure 3: Log-log plot of mass versus volume modulus in the regime  $e^{\frac{1}{4}} < c < e^{\frac{1}{4}A_0}$ . Mass is measured in units of the warped KK scale  $e^{A_0} = R$ . Points represent the lightest masses calculated in appendix B. The black best-fit lines have slopes  $-0.01$ ,  $-0.49$ , and  $-24$  respectively. The dashed line is the mass predicted by semiclassical bulk arguments for  $c = e^{A_0}$ ,  $m = m_f = c$ .

with the role of  $c$  as a radial modulus. As we saw in section 2, the flux-induced mass is constant in the throat but is suppressed by the warp factor in the bulk:

$$m_f^2(r) = \begin{cases} m_f^2 & (r_0 < r < r_c) \\ m_f^2 = c^{3/2} & (r_c < r < r_c + \frac{p}{c}) \end{cases} ; \quad (3.38)$$

where  $m_f = \frac{p}{g_s n_f} = \frac{p}{c}$  is a constant mass. This formula for the mass represents the extreme possibility that the dilaton-axion feels the same flux in the bulk and throat regions.

In terms of the Schrodinger equation (3.22), we find  $x = R^2 = r$  in the throat region and  $x = 2x_c \frac{p}{c} = r$  in the bulk region, with  $x_c = R^2 = r_c = c^{1/4} R$ . Signs and integration constants have been chosen so that the coordinate  $x$  is continuous as a function of  $r$ . For states with no angular momentum, the potential is

$$V(x) = \frac{1}{x^2} - \frac{15}{4} + m_f^2 R^2 \left( (x - x_c) + \frac{m_f^2}{c^2} (x_c - x) + (x - x_c) \frac{x}{R} \right)^{3/2} \partial_x \left( \frac{R}{x} \right)^{3/2} ; \quad (3.39)$$

The final term requires that

$$\psi(x) \text{ and } \partial_x e^{3A/2} \psi(x) \quad (3.40)$$

are continuous at the boundary point  $x_c$ . These boundary conditions are consistent with (3.21) for a continuous warp factor. We also impose Neumann boundary conditions on  $\psi = e^{3A/2}$  at the endpoints  $x_c \frac{p}{c}$  and  $x_0$ .

We have calculated the lightest mass for this potential as a function of bulk size  $c$  for a fixed warp factor  $e^{A_0}$  and flux-induced mass  $m_f$ . Since the throat region disappears for  $c \geq e^{4A_0}$  and the bulk should be at least string scale, we consider only  $1 \leq c \leq e^{4A_0}$ . We leave the details of the calculation for appendix B, but we present the basic results here.

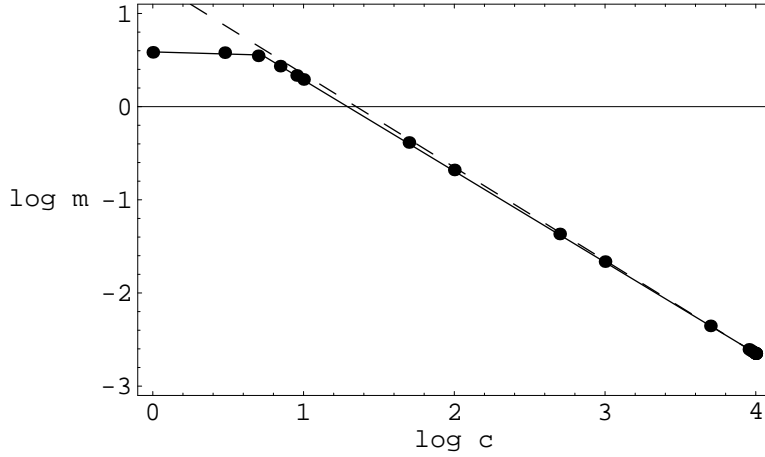


Figure 4: Log-log plot of mass versus volume modulus, as in figure 3. The best-fit lines have slopes -0.05 and -0.98 respectively.

First, referring to figure 3, we see that the lightest modes for  $c < e^{A_0}$  do have mass  $m \sim m_f e^{A_0}$ , nearly independent of the overall compactification volume  $c$ . These modes are localized, but it is easy to check that they delocalize when  $c \gg e^{A_0}$ , just as we expect from the discussion of section 3.3. However, the delocalized bulk modes have masses that scale like  $m \propto 1/c^{p_-}$  rather than  $m \propto 1/c$ , as we expect from our semiclassical intuition. Then the masses drop sharply to  $m \sim m_f = c$  just before the throat disappears ( $c \sim e^{4A_0}$ ). We should note that this interesting behavior is almost certainly model-dependent, but the main point is that the intermediate behavior indicates that the quantum mechanics of the potential (3.39) are important for some values of the compactification volume.

Because the flux described in the KS background cannot freeze the dilaton by itself [1], it is possible that the flux-induced mass parameter differs in the bulk and the throat (or perhaps decays as the warp factor decreases). To check that our qualitative results are not altered, we have also calculated the lightest mode masses in the same geometry with

$$m_f^2(r) = \begin{cases} 0 & (r_0 < r < r_c) \\ m_f^2 = c^{3-2p_-} & (r_c < r < r_c + \epsilon) \end{cases} : \quad (3.41)$$

This is the extreme case that the dilaton-axion feels no flux in the throat region. In this case, we again find that the lightest mode masses are constant with  $c$  and approximately  $m \sim m_f e^{A_0}$  for  $c \ll e^{A_0}$ , just as we expect from semiclassical reasoning. Then, for larger  $c \gg e^{A_0}$ , the lightest modes have mass given by the semiclassical bulk result  $m \sim m_f = c$ . See figure 4. Interestingly, the lightest modes never delocalize in the sense that they always decay in the bulk; however, for  $c \gg e^{A_0}$ , the decay is negligible, and the wavefunction is almost flat in the bulk. Additionally, the KK wavefunction is much larger in the bulk than the throat, so the modes have essentially delocalized. See appendix B for a discussion of the wavefunctions.

The chief result of these calculations is that, by and large, semiclassical physics is sufficient, although, in realistic models, quantum effects may be relevant in the intermediate region  $e^{A_0} \lesssim c \lesssim e^{4A_0}$ . Most importantly, the wavefunctions are localized in the throat region for  $c \lesssim e^{A_0}$ , where the mass is given by the warped scale,  $m \sim m_f e^{A_0}$ .

In appendix B, we also discuss the Kaluza-Klein mass gap for the dilaton given a range of compactification parameters. In case of either flux-induced mass function (3.38) or (3.41), we get similar results for the KK mass gap for the lowest mass states:

$$c \lesssim e^{2A_0} \Rightarrow m_n \sim \frac{e^{A_0}}{R} \quad (3.42)$$

and

$$c \gtrsim e^{2A_0} \Rightarrow m_n \sim \frac{1}{c^{1/2}} : \quad (3.43)$$

In the long throat ( $c \lesssim e^{A_0}$ ) regime, the gap (3.42) is every important, since the lightest mode has a mass of the same order as the KK mass gap. In other words, it may be impossible to describe moduli stabilization through an effective superpotential for compactifications with long throats — we must integrate out the stabilized moduli at the same time as KK modes. A similar concern arises for the smaller KK mass gap (3.43) if the lowest mass follows the pattern of figure 3, when the lightest mass will be of the same order as the mass gap. While our results only follow from clearly rough models of the physics, they do caution that we may not be able to describe moduli stabilization in effective theory when throats exist ( $c \lesssim e^{4A_0}$ ) or are long ( $c \lesssim e^{A_0}$ ). We also find in appendix B that it is possible to have, for large  $m_f$ , a KK mass gap of  $m \sim 1/m_f^{1/2}$  at small  $c$ , which is suppressed from the string scale by the flux quanta. However, this can only occur when  $m_f^{1/2} \sim R \lesssim e^{A_0}$ .

#### 4. Discussion

In this section, we will review our findings and discuss their implications for both the theory and phenomenology of flux compactifications in string theory. As a brief review, we recall that we have found that the lowest dilaton-axion KK mode wavefunction localizes in deep throats — those for which  $e^{A_0} \lesssim c$ . These localized modes have masses  $m \sim \frac{e^{A_0}}{R^{1/2}}$ . For larger compactifications,  $c \gtrsim e^{A_0}$ , the mass decreases (see figures 3 and 4). Semiclassically, we expect  $m \sim \frac{1}{c^{1/2}}$ , which is the result in the infinite volume limit  $c \lesssim e^{4A_0}$ , in which the throat disappears. The semiclassical behavior may or may not hold for  $c \lesssim e^{4A_0}$ ; in one of our examples, the mass scales like  $c^{1/2}$ , similar to a bulk KK mode. We have also estimated the effect of compensators on the dilaton-axion mass, and we found that they give a negligible contribution in the bulk and sufficiently long throats. Our results were derived using simple models, which nonetheless seem to encapsulate key features of the corresponding string compactifications.

First, our results are important for determining which degrees of freedom should be included in the four-dimensional effective theory describing the compactification. The regime

of validity of the effective theory is given by the scale of the KK excitations (since it describes the dynamics with these degrees of freedom integrated out). In the deep throat regime, we found that there is no hierarchical separation between the dilaton mass and its KK scale. In fact, following [18, 20, 29, 30], we expect that the KK excitations of the 4D graviton will also have masses of this same scale. Therefore, we expect that all the dilaton-axion should be integrated out of the effective theory in the deep throat regime ( $c \ll e^{A_0}$ ).

On the other hand, the dilaton mass and KK scale separate at larger compactification volume. Following our semiclassical analysis, we expect a dilaton mass  $m_z = \frac{1}{c} \frac{1}{p} \frac{1}{\ell^0}$  in the short-throat and no-throat regime. This compares to a KK mass scale of  $e^{A_0} = \frac{1}{p} \frac{1}{\ell^0}$  (for  $c \ll e^{2A_0}$ ) or  $m_z = \frac{1}{c} \frac{1}{\ell^0}$  (larger  $c$ ). In this case, the dilaton-axion need not be integrated out of the effective theory. We do caution that semiclassical reasoning may fail for  $e^{A_0} \sim c \ll e^{4A_0}$ , in which case the two scales may not be hierarchically separated.

So far, we have focused on the dilaton-axion. Widening our view a bit, the equations describing the fluctuations of the metric moduli have also been obtained in [14]. These equations are quite complicated, and we are unable to analyze them in detail at present. However, they are qualitatively similar to the equation for the fluctuation of the dilaton-axion. In particular, the structure is compatible with solutions which are oscillatory in a throat region and damped in the bulk. This suggests that some (or all) of the metric moduli might also exhibit the localization we have discussed for the dilaton.

In fact, we expect very similar behavior for complex structure moduli. In the infinite volume limit, the geometry is same as that of the conventional Calabi-Yau construction. In this regime, the equations for linearized fluctuations obtained in [14] are easily analyzed, and the mass is just  $m_z = \frac{1}{c} \frac{1}{p} \frac{1}{\ell^0}$ . As the compactification volume is decreased and a long throat develops, one expects the wavefunctions to change; becoming highly localized in the throat region. The masses would then redshift to  $m_z = e^{A_0} = \frac{1}{p} \frac{1}{\ell^0}$ . The details will most likely depend on the mode in question and are beyond the scope of our analysis, so it is possible that some moduli will not fit this pattern, in which case they are more massive than KK modes in the deep throat regime. However, the fact that the dilaton — whose wavefunction is uniform in the infinite volume limit — localizes indicates that this behavior might be fairly generic.

The dynamics of moduli is crucial for understanding physics related to the hidden sector. In the context of IIB compactifications, it can be argued that the superpotential generated by the fluxes is that of Gukov, Vafa, and Witten [15],

$$W = \int_{\Sigma} G \wedge \Omega \quad (4.1)$$

This superpotential describes the effective field theory of the dilaton-axion and complex structure moduli, with higher Kaluza-Klein modes integrated out. We have argued that if one starts at the infinite volume limit and continuously decreases the volume, the wavefunctions of the dilaton and possibly some of the metric moduli continuously localize to the bottom of the longest throat. Given the non-renormalization properties of the superpotential, we expect it

to be relevant for the dynamics of modes localized in the deepest throat, rather than bulk modes or modes localized in other throats.

While the superpotential is thought to be unaffected by the warp factor, our results show that warping corrects the Kähler potential. Taking the uncorrected Kähler potential of an orientifold Calabi-Yau compactification just gives a mass  $m_{n_f=c} = \frac{1}{c} \frac{1}{\sqrt{\alpha'}}$  for the dilaton-axion. However, as we have seen, the lowest dilaton mass is given by the warped string scale  $m_{n_f=c} = \frac{1}{c} \frac{1}{\sqrt{\alpha'}} e^{A_0}$  when there are long throats, so the Kähler potential must be corrected. Since we have argued that compensators should give only small contributions to the mass, a possible Kähler potential is that proposed in [21], with suitable modifications due to corrected holomorphic coordinates, as suggested in [14]. We should caution, though, that the dilaton-axion (and complex structure moduli) may be too heavy for the effective theory, in which case only classically massless fields would appear in the Kähler potential.

Our findings are also important in understanding the nature of couplings between the standard model and the supergravity sectors in brane world scenarios. Consider a scenario in which the standard model branes are located at the bottom of a deep throat, with the hierarchy problem solved as proposed by Randall and Sundrum. In such a scenario, our calculations suggest that the mass of the bulk modes would also be in the TeV scale, so we would expect couplings of order unity between supergravity and matter fields at the TeV scale. This is analogous to the findings of Goldberger and Wise in [16]. The phenomenological implications for a scenario in which the standard model branes are located in the bulk of a compactification with a deep throat are also interesting. In this case, the wavefunctions of the moduli are highly suppressed in the bulk region, and their couplings to the standard model branes would be very weak. However, it would be interesting to examine the collective effect on the of the large number of localized modes on the bulk to brane coupling. In terms of string compactifications, D 7-branes intersecting in the bulk could provide the standard model degrees of freedom.

We can also consider cosmological consequences of these results. For example, KKLT [31] models see common use in brane-antibrane inflation scenarios (see, for example, [32–35]). The key element in these models is an anti-D 3-brane present at the bottom of a KS-like throat, and the inflationary potential is given by the redshifted brane tension. In a high-scale inflation model, it is reasonable to expect a hierarchy of  $e^{A_0} \sim 10^3$  and  $c^{1/4} \sim 10$ , where  $c^{1/4}$  is also the linear scale of the bulk. This clearly falls into the short throat regime we have discussed, in which the dilaton mass is less than the warped KK scale. Reheating bulk modes would also provide a mechanism to reheat the standard model if it were located on D 7-branes wrapping a bulk cycle. In terms of inflation, there are also consequences for multi-throat models discussed in [36–38]. As [39] has argued, light degrees of freedom in a second throat could shorten that throat, reducing its hierarchy. Our results strengthen that conclusion by arguing that frozen moduli do have redshifted masses in long throats. Also as discussed in [39], the evolution of these light moduli could lead to an additional stage of reheating, and it remains to be seen whether a moduli overproduction problem could occur.

Let us also mention KKLT models [31] in the context of the cosmological constant. In



We close with a brief comment on future directions. An obvious extension of our work is to more realistic models of the geometry. For example, [40] gives a better approximation of the KS geometry. Another important direction would be to extend our analysis to other complex structure moduli, as in [41]. Also, in KKLT models, the overall volume is stabilized by introducing energy sources localized on certain submanifolds in the bulk of the Calabi-Yau. It would be interesting to study the nature of the wavefunction and the mass of the lowest mode after the introduction of such sources.

The authors would like to thank A. Basu, I. Bena, H. Elvang, S. Giddings, S. Gukov, N. M. Ann, P. Ouyang, J. Polchinski, A. Sen, and A. Virmani for useful discussions and communications. The work of ARF is supported by the John A. McOne postdoctoral fellowship at the California Institute of Technology and also partially by the Department of Energy contract DE-FG03-92-1ER40701. The work of AM is supported by the Department of Energy under contract DE-FG02-91ER40618. AM would like to thank the Hebrew University for hospitality during the 23rd Jerusalem Winter School.

In this appendix, we detail our estimate of the effects of compensators on the dilaton-axion mass and wavefunction. Since the NSNS and RR sectors decouple and the equations have the same form in both sectors, we work only with the NSNS sector equations (3.15) (remember that we are setting the angular momentum to zero on the internal 5 dimensions). Following the logic leading to the Schrodinger-like form (3.22) of the dilaton-axion equation of motion, we can rewrite (3.15) as the eigenvalue equation

with "Hamiltonian" and perturbation

{ 24 {

The  $\partial_x$  in the perturbation Hamiltonian indicates that the derivative should act on the wavefunction as well as the explicit factor.

The other important contribution to the problem comes from the boundary conditions. We have Neumann boundary conditions for  $\phi$  at both ends of the throat, meaning

$$\partial_x \left( \frac{x}{R} \right)^{3/2} \phi(x_0) = \partial_x \left( \frac{x}{R} \right)^{3/2} \phi(R) = 0 : \quad (\text{A.3})$$

The 2-form potential satisfies the same Neumann boundary conditions in the IR end of the throat  $x_0$ , but we take it to satisfy Dirichlet boundary conditions at the UV end  $x = R$ :

$$\partial_x \left( \frac{x}{R} \right)^{3/2} B(x_0) = 0 ; \quad B(R) = 0 : \quad (\text{A.4})$$

This Dirichlet boundary condition simulates the odd parity of  $B$  under the orientifold 3-plane or 7-plane projection around a point in the bulk. Using (3.26), we find the unperturbed eigenstates

$$\begin{aligned} \psi_{j;n} &= \left( \frac{x}{R} \right)^{3/2} (C_1 J_q(m x) + C_2 Y_q(m x)) \\ \mathcal{B}_{j;n} &= \left( \frac{x}{R} \right)^{3/2} (D_1 J_2(m_B x) + D_2 Y_2(m_B x)) \end{aligned} \quad ; \quad (\text{A.5})$$

where  $q$  is defined in (3.26) and  $n$  indicates the excitation number in the  $x$  direction. The coefficients are related to each other by the  $x = R$  boundary conditions:

$$\frac{C_2}{C_1} = \frac{2J_q(m R) + m R J_q^0(m R)}{2Y_q(m R) + m R Y_q^0(m R)} ; \quad \frac{D_2}{D_1} = \frac{J_2(m_B R)}{Y_2(m_B R)} : \quad (\text{A.6})$$

The masses are determined by transcendental equations obtained from applying (A.6) to the  $x = x_0$  boundary conditions [16].

Despite the fact that the perturbation Hamiltonian is not hermitian, usual perturbation theory still applies, as in quantum mechanics. Normalizing our wavefunctions to unity when integrated over  $x$ , we find a second-order contribution to the lowest dilaton mass

$$(m^2) = \sum_n \frac{\langle \psi_{j;n} | H | \mathcal{B}_{j;n} \rangle \langle \mathcal{B}_{j;n} | H | \psi_{j;0} \rangle}{m^2 - m_{B,n}^2} : \quad (\text{A.7})$$

For a fixed hierarchy  $e^{A_0} = x_0/R = 10^3$ , we have shown by direct calculation that the two lowest modes of  $B$  dominate the correction to the dilaton mass-squared. Also, given the behavior of the terms we have checked explicitly, the sum appears to be well behaved and convergent. Throughout our calculations, we have set  $n_h = 1$  and  $m_f R = 3$ .

We now want to study the dependence of  $(m^2)$  on the warped hierarchy  $e^{A_0}$ . To do so, we calculated the sum (A.7) for the two lowest modes of  $B$  at five different values for the minimum warp factor. At these hierarchies, we find

$$\frac{(m^2)}{m^2} / e^{A_0} : \quad (\text{A.8})$$

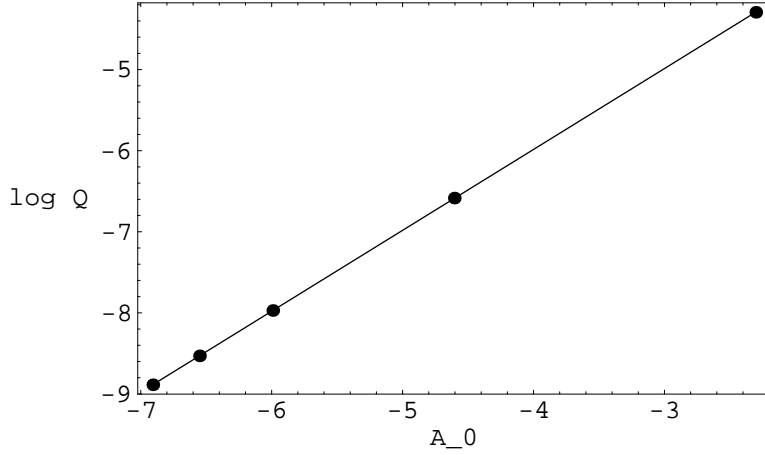


Figure 5: Change in mass-squared versus minimal warp factor  $A_0$ .  $Q = j(m^2) = m^2 j$ . Points are calculated values, and the line is the best-fit  $\ln Q = 0.998 A_0 - 1.99$ .

This scaling is shown in figure 5. This rather clean scaling behavior is somewhat of a surprise, given the number of truncations and assumptions we have made in arriving at our estimated  $(m^2)$ . It is certainly an intriguing idea that the full effect of the compensator might obey a simple scaling law with the warped hierarchy. Finally, given that the effect of the compensator is quite small (as can be seen from the figure) even for relatively mild hierarchies, we will ignore the effects of compensators throughout the rest of the paper.

## B. Throat Plus Bulk Calculations

In this appendix, we give specifics of calculations needed to understand models with both throat and bulk regions, with the warp factor given in equation (3.37) and flux-induced mass parameter given in (3.38, 3.41). We consider the case of vanishing angular momentum ( $Q = 0$ ) for simplicity.

In the throat region, the wavefunction is given by Bessel functions as in (3.26):

$$\psi(x) = \frac{r}{R} J_{\frac{x}{R}}(m_n x) + b_n \frac{r}{R} Y_{\frac{x}{R}}(m_n x) : \quad (\text{B.1})$$

Depending on the flux that couples to the dilaton in the throat, we have

$$= \frac{q}{4 + m_f^2 R^2} \text{ or } = 2 : \quad (\text{B.2})$$

By imposing Neumann boundary conditions at  $x_0$  (the bottom of the throat), we find

$$b_n = \frac{2J_{\frac{x}{R}}(m_n x_0) + m_n x_0 J_{\frac{x}{R}}^0(m_n x_0)}{2Y_{\frac{x}{R}}(m_n x_0) + m_n x_0 Y_{\frac{x}{R}}^0(m_n x_0)} : \quad (\text{B.3})$$

In the bulk region, imposing Neumann boundary conditions at  $x_c$   $\frac{p}{c} \rightarrow 0$  gives two possible solutions

$$\begin{aligned} \psi(x) = B_n & \begin{cases} \cosh \frac{h q \sqrt{m_f^2 - c^2}}{m_n^2} x & x < x_c + \frac{p}{c} \rightarrow 0 \\ \cos \frac{h q \sqrt{m_n^2 - m_f^2}}{m_n^2} x & x > x_c + \frac{p}{c} \rightarrow 0 \end{cases} \quad (m_n = m_f = c) \end{aligned} \quad (B.4)$$

The boundary conditions (3.40) at  $x_c$  are therefore satisfied when

$$f(z_n) = 2e^H + z_n \frac{(2Y(z_n) + z_n Y^0(z_n))J^0(z_n e^H)}{(2Y(z_n) + z_n Y^0(z_n))J(z_n e^H)} = \frac{(2J(z_n) + z_n J^0(z_n))Y^0(z_n e^H)}{(2J(z_n) + z_n J^0(z_n))Y(z_n e^H)} \quad (B.5)$$

equals

$$q \frac{1}{m_f^2 x_0^2 - c^2} z_n^2 \tanh \frac{p}{c} \frac{1}{x_0} \quad (B.6)$$

or

$$q \frac{1}{z_n^2 - m_f^2 x_0^2 - c^2} \tan \frac{p}{c} \frac{1}{x_0} \quad ; \quad (B.7)$$

where  $z_n = m_n x_0$ .

We have found numerically the lightest mass modes for the fixed values  $m_f = \frac{p}{5}$ ,  $e^{A_0} = 1=10$ , and  $\frac{p}{c} \rightarrow 0 = e^{A_0}$ , and allowing the size of the bulk  $c$  (and therefore the hierarchy  $e^H$ ) to vary from 1 to  $e^{4A_0}$ . We end the results presented in section 3.4. We also present here (figure 6) the wavefunctions of the lightest mass modes for several different values of the volume modulus  $c$ . In particular, note that the wavefunctions are suppressed in the throat region ( $x > x_c$ ) for  $c \ll e^{A_0}$ , but that only the case in which  $m_f(x) \neq 0$  in the throat yields an oscillatory wavefunction in the bulk.

Let us also discuss the mass spacing of KK modes in these two models. A typical solution (note that the lowest solution  $z_0$  may very well be atypical) to the boundary condition (3.40) occurs near a singularity of either  $f(z)$  defined in (B.5) or the tangent (B.7), so the KK mass gap is defined by the spacing of singularities of those two functions. The singularities of  $f(z)$  are spaced by  $z \approx 1$  from our knowledge of Bessel functions, and numerical work shows that the spacing is indeed around 4 or 5. This spacing leads to a mass gap of order  $m_n \approx 1/x_0 = e^{A_0}/R$ , which is the redshifted curvature scale for the throat. On the other hand, the tangent (B.7) has singularities when

$$q \frac{1}{z^2 - x_0^2 - m_f^2 - c^2} \frac{p}{c} \rightarrow 0 = \frac{p}{2} \quad ; \quad p \approx 2(2Z + 1) \quad (B.8)$$

Differentiating, we can approximate

$$z \approx \frac{p^2 x_0}{2c} \frac{p^2}{4c} + \frac{m_f^2}{c^2} \quad ; \quad (B.9)$$

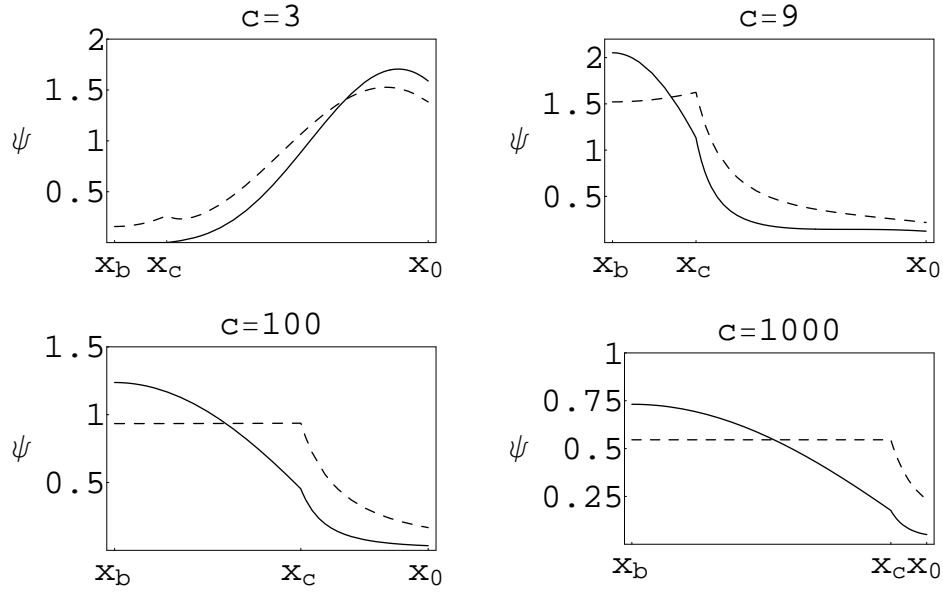


Figure 6: Wavefunctions for 4 values of  $c$ . The solid curves are for  $m_f(x) \neq 0$  in the throat, while the dashed are for  $m_f(x) = 0$  in the throat. For comparison, the wavefunctions have been normalized as  $\int_{x_b}^{x_0} dx \psi^2 = 1$ . In the figures,  $x_b = x_c - \frac{1}{c}$ . Note that the throat gets shorter and the bulk longer as  $c$  increases.

There are two regimes for this solution:

$$z = \frac{x_0}{c} \quad \left( m_f^2 \leq \frac{c^2}{4} \right) \quad (\text{B.10})$$

$$z = \frac{\sqrt{2}x_0}{m_f} \quad \left( m_f^2 > \frac{c^2}{4} \right) : \quad (\text{B.11})$$

Since the smallest spacing of singularities determines the KK mass gap, this last value (B.11) is only important for  $m_f \neq 0$  &  $x_0$ , or  $m_f = 0$  &  $e^{A_0} = R$  (consider the comparison to the singularity spacing of  $f(x)$ ). Because the throat curvature radius  $R$  is determined by the flux (as is  $m_f$ ), we may expect  $m_f = R^{-1}$ , although it is possible that (B.11) becomes relevant for a Calabi-Yau with a large number of 3-cycles on which the flux can wrap (and sufficiently small volume modulus  $c$ ). These two spacings give KK mass gaps of

$$m_n = \frac{1}{c} \quad \text{or} \quad m_n = \frac{1}{m_f} \quad (\text{B.12})$$

respectively. These are the unwarped bulk KK scale and an almost string scale mass — it is suppressed by the amount of flux.

Comparing the singularity spacings given above, the KK mass gap (without large  $m_f$ ) is the warped KK scale of the throat  $m = e^{A_0}/R$  for small  $c$ .  $e^{2A_0}$  transitioning to the bulk KK scale  $m = 1/c$  if the compactification radius is increased sufficiently. At large

ux-induced mass  $m_f$ , the KK mass gap is  $m_{1=0} = m_f$  at small volume modulus and  $m_{1=0} = \frac{p}{c}$  at large volume.

Finally, we should mention that it is straightforward to check that there are no massless modes in the potential (3.39) for  $m_f \neq 0$ . The unnormalized wavefunction in the throat would be

$$\psi(x) = x^{1=2} + \frac{2}{2+} x_0^2 x^{1=2+}; \quad (B.13)$$

The coefficient on the second term comes from imposing Neumann boundary conditions on  $\psi$  at  $x_0$ . The wavefunction in the bulk region is the hyperbolic cosine above with  $m_n = 0$ . The boundary conditions at  $x_c$  then imply

$$\frac{m_f}{c} \tanh \frac{p}{m_f} \frac{p}{c} = (4 - 2) \frac{1 + (x_0=x_c)^2}{(2 - )x_0 + (2 + ) (x_0=x_c)^2 x_c} : \quad (B.14)$$

This matching condition is inconsistent because  $-2$  for nonzero  $m_f$  (or angular momentum, for that matter). The left-hand side is positive definite, and the right-hand side can be positive only when the denominator is negative, or

$$\frac{-2 + 2 \frac{x_0}{x_c}}{2 \frac{x_0}{x_c}} < 1; \quad (B.15)$$

which is impossible because  $x_0 > x_c$ .

## References

- [1] S.B. Giddings, S. Kachru and J. Polchinski, Phys. Rev. D 66, 106006 (2002), [hep-th/0105097].
- [2] S. Kachru, M. B. Schulz and S. Trivedi, JHEP 10, 007 (2003), [hep-th/0201028].
- [3] A. R. Frey and J. Polchinski, Phys. Rev. D 65, 126009 (2002), [hep-th/0201029].
- [4] P. K. Tripathy and S. P. Trivedi, JHEP 03, 028 (2003), [hep-th/0301139].
- [5] A. Giryavets, S. Kachru, P. K. Tripathy and S. P. Trivedi, JHEP 04, 003 (2004), [hep-th/0312104].
- [6] I. Antoniadis, A. Kumar and T. Maillard, hep-th/0505260.
- [7] D. Lust, S. Rebertus, W. Schulgin and S. Stieberger, hep-th/0506090.
- [8] A. R. Frey, hep-th/0308156.
- [9] E. Silverstein, hep-th/0405068.
- [10] M. G. Pospelov, Phys. Rept. 423, 91 (2006), [hep-th/0509003].
- [11] S. P. de Alwis, Phys. Rev. D 68, 126001 (2003), [hep-th/0307084].
- [12] A. Buchel, Phys. Rev. D 69, 106004 (2004), [hep-th/0312076].
- [13] S. P. de Alwis, Phys. Lett. B 603, 230 (2004), [hep-th/0407126].
- [14] S. B. Giddings and A. Maharana, hep-th/0507158.

- [15] S. Gukov, C. Vafa and E. Witten, Nucl. Phys. B 584, 69 (2000), [hep-th/9906070].
- [16] W. D. Goldberger and M. B. Wise, Phys. Rev. D 60, 107505 (1999), [hep-ph/9907218].
- [17] L. Randall and R. Sundrum, Phys. Rev. Lett. 83, 3370 (1999), [hep-ph/9905221].
- [18] H. Firouzjahi and S.-H. H. Tye, JHEP 01, 136 (2006), [hep-th/0512076].
- [19] T. Noguchi, M. Yamaguchi and M. Yamashita, hep-th/0512249.
- [20] X. Chen and S.-H. H. Tye, hep-th/0602136.
- [21] O. DeWolfe and S. B. Giddings, Phys. Rev. D 67, 066008 (2003), [hep-th/0208123].
- [22] I. R. Klebanov and M. J. Strassler, JHEP 08, 052 (2000), [hep-th/0007191].
- [23] C. P. Herzog, I. R. Klebanov and P. Ouyang, hep-th/0108101.
- [24] C. P. Herzog, I. R. Klebanov and P. Ouyang, hep-th/0205100.
- [25] I. R. Klebanov and A. A. Tseytlin, Nucl. Phys. B 578, 123 (2000), [hep-th/0002159].
- [26] S. Franco, A. Hanany and A. M. Uranga, JHEP 09, 028 (2005), [hep-th/0502113].
- [27] A. R. Frey and A. Mazumdar, Phys. Rev. D 67, 046006 (2003), [hep-th/0210254].
- [28] C. Saki, J. Erlich, T. J. Hollowood and Y. Shimizu, Nucl. Phys. B 581, 309 (2000), [hep-th/0001033].
- [29] J. D. Lykken, R. C. Myers and J. Wang, JHEP 09, 009 (2000), [hep-th/0006191].
- [30] L. Randall and R. Sundrum, Phys. Rev. Lett. 83, 4690 (1999), [hep-th/9906064].
- [31] S. Kachru, R. Kallosh, A. Linde and S. P. Trivedi, Phys. Rev. D 68, 046005 (2003), [hep-th/0301240].
- [32] S. Kachru et al., JCAP 0310, 013 (2003), [hep-th/0308055].
- [33] C. P. Burgess et al., JHEP 07, 047 (2001), [hep-th/0105204].
- [34] H. Firouzjahi and S.-H. H. Tye, Phys. Lett. B 584, 147 (2004), [hep-th/0312020].
- [35] C. P. Burgess, J. M. Cline, H. Stoica and F. Quevedo, JHEP 09, 033 (2004), [hep-th/0403119].
- [36] N. Barnaby, C. P. Burgess and J. M. Cline, JCAP 0504, 007 (2005), [hep-th/0412040].
- [37] L. Kofman and P. Yi, Phys. Rev. D 72, 106001 (2005), [hep-th/0507257].
- [38] D. Chialva, G. Shiu and B. Underwood, JHEP 01, 014 (2006), [hep-th/0508229].
- [39] A. R. Frey, A. Mazumdar and R. Myers, Phys. Rev. D 73, 026003 (2006), [hep-th/0508139].
- [40] P. Langfelder, hep-th/0602296.
- [41] S. B. Giddings and P. Ouyang, work in progress.